acta physica slovaca vol. 45 No. 1, 45 – 55 February 1995

NONCOLLINEAR MAGNETIC STRUCTURES INVESTIGATED BY HIGH-FIELD MÖSSBAUER SPECTROMETRY[1]

Jean-Marc Greneche[2]
Equipe de Physique de l'Etat Condensé, URA CNRS 807 Université du Maine
F72017 Le Mans Cedex France

Received 8 December 1994, accepted 23 December 1994

Some experimental and theoretical aspects of High Field Mössbauer Spectrometry are briefly presented, as well as its applications, essentially focused to magnetic iron-based compounds. Then, we report on some selected examples of High Field Mössbauer studies performed on various crystalline and amorphous ferric fluorides, which gave evidence for noncollinear magnetic arrangements due to the presence of topologically frustrated antiferromagnetic interactions.

1. Introduction

Actually, High Field Mössbauer Spectrometry [HFMS] is more frequently used in the laboratories because various technological developments have been done over the two last decades. In conjunction with usual Mössbauer experiments, the application of a magnetic field to a conventional spectrometer provides a wealth of relevant information relative to the structural, electronic and magnetic properties of solids. Let us mention that the first experiment was performed in 1960 by Hanna et al [1]: this group determined the sign of the hyperfine field in α-Fe using a field of 20k0e produced by a conventional electromagnet.

Static magnetic field up to 15T can be currently produced either by superconducting magnets or Bitter magnets. The samples are located either in low temperatures dewars as cryomagnetic devices and dilution refrigerators or at high temperatures using vacuum furnace inside superconducting coils. Some review papers have been previously devoted to HFMS applications [2, 3, 4, 5].

After a brief presentation of the different kinds of information which can be obtained by HFMS, we illustrate its contribution to the determination of non collinear magnetic structures, supported by several examples taken among ferric fluorides. Non collinear

[1]Presented at the Colloquium on Mössbauer Spectroscopy in Material Science, Kočovce, Slovakia, October 3-6, 1994

[2]E-mail address: greneche@univ-lemans.fr

0323-0465/95

magnetic arrangements originate from the presence of competing interactions either in crystalline [6] or in amorphous [7] magnetic systems.

During the last decade, new forms of transition metal fluorides which have been successfully synthetized according to different methods as hydrothermal, chemical vapour deposition and "chimie douce", exhibit rather interesting crystallographic and magnetic structures. Because magnetic frustration arises with antiferromagnetic interactions whenever the magnetic lattice possesses odd-membered rings as triangular platelets [8], the cationic topology of some fluoride compounds originates frustrated antiferromagnetic interactions between first nearest neighbors, and consequently, induces noncollinear magnetic arrangements (see some reviews in [9, 10]).

2. Why HFSM?

By applying a magnetic field H_{app} on a sample characterized by $\mathcal{H}_0$, the nuclear system can be described by a hamiltonian which is generally expressed as

$$\mathcal{H} = \mathcal{H}_0 + \mathcal{H}_M. \tag{1}$$

$\mathcal{H}_0$ characterizes the system out of field and $\mathcal{H}_M$ represents the Zeeman term. $\mathcal{H}_0$ results from the sum of different contributions:

$$\mathcal{H}_0 = \mathcal{H}_{hf} + \mathcal{H}_{FI} + \mathcal{H}_{CF} + \mathcal{H}_{Exc} + \mathcal{H}_{dd} + \mathcal{H}_d + \mathcal{H}_{QL} + \mathcal{H}_{Thf} \tag{2}$$

One can distinguish (i) intra-atomic terms $\mathcal{H}_{hf}$ with magnetic and quadrupole origins, (ii) electronic atomic term $\mathcal{H}_{FI}$ (free-ion contribution) and (iii) electronic inter- atomic terms (crystal field $\mathcal{H}_{CF}$, exchange $\mathcal{H}_{Exc}$ and magnetic dipole-dipole interaction $\mathcal{H}_{dd}$), as well as (iv) smaller contributions as dipolar interactions of the spin neighbours with the nucleus $\mathcal{H}_d$, the lattice electric field gradient $\mathcal{H}_{QL}$ or transferred magnetic field H_{Thf}, resulting from the transfer of spin density at the nucleus.

In (2), the intra-atomic hyperfine term is expressed by $\mathcal{H}_{hf} = \mathcal{I}[A]\mathcal{S} + Q\nabla E^{Val}$, where $\mathcal{I}$ is the nuclear spin, $[A]$ the hyperfine tensor, $\mathcal{S}$ the effective spin operator and where Q represents the quadrupole moment, ∇E^{Val} is the valence contribution to the electric field gradient. The magnetic contribution can be written as $-\gamma_N\hbar\mathcal{I}H_{int}$ where H_{int} is the internal field which is often confused with the hyperfine field H_{hyp}.

The Zeeman term $\mathcal{H}_M$ in (1) is expressed by

$$\mathcal{H}_M = -g\mu_B\hbar\mathcal{S}H_{app} - \gamma_N\hbar\mathcal{I}H_{app} = -MH_{app} - \gamma_N\hbar\mathcal{I}H_{app} \tag{3}$$

where $g\mu_B\hbar\mathcal{S}$ and $\gamma_N\hbar\mathcal{I}$ are the operators corresponding to the electronic and nuclear magnetic moment, respectively, and M corresponds to the magnetization.

The nucleus of the diamagnetic probe atom becomes "passive" in the presence of an external field, and the measured effective field is equal to H_{app}. For paramagnetic compounds, the shape of the in-field Mössbauer spectra depends strongly on the electronic relaxation time as compared with nuclear Larmor period; the analysis of the in-field spectra contributes to the estimation of the crystal field parameters and to the determination of the sign of the electric field gradient.

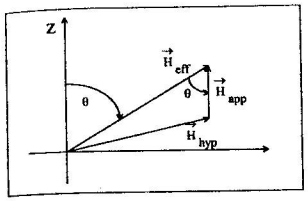

Figure 1: Schematic arrangement of the hyperfine field H_{hyp}, the effective field H_{eff} and the applied field H_{app} which act at a nucleus (Z is the quantization axis).

As the magnetic hyperfine contribution is defined by $\mathcal{I}[A]\mathcal{S}$, the application of an external field leads to

$$\mathcal{H} = \mathcal{I}[A]\mathcal{S} - g_N\beta_N H_{app}\mathcal{I} \tag{5}$$

with g_N and β_N are the nuclear g factor and the nuclear Bohr magneton, respectively.

When considering large external fields, $g_N\beta_N H_{app} >> [A]\mathcal{S}$ and the spins are quantized along the direction of the external field; in that way, off-diagonal terms can be neglected. Consequently, one can define an effective field H_{eff} which acts on the nucleus, such that

$$H_{eff} = H_{app} - [A]\langle S\rangle/g_N\beta_N. \tag{6}$$

In addition, the effective field results from the vectorial sum of the hyperfine field and of the applied field, as illustrated in figure 1; so,

$$\vec{H}_{eff} = \vec{H}_{app} + \vec{H}_{hyp} \tag{7}$$

The most common situation is obtained in the case of magnetic compounds. The pertinent parameters are related to the shape, the splitting and the intensities of the absorption Zeeman lines and the value of the measured effective field has to be compared to that of the hyperfine field in order to determine their relative orientation. The theoretical Mössbauer spectra expected for different typical magnetic arrangements are illustrated in figure 2.

In the case of ferric ions, the hyperfine tensor $[A]$ becomes a scalar because of the isotropic behavior of Fe^{3+} (^6S). As the hyperfine field results essentially from the contact Fermi term (due to the polarization of the core-s electrons by the magnetized $3d$ electrons), the hyperfine field is close to be proportional to the spin of the ion, i.e. the magnetization. So, the in-field Mössbauer spectra provide valuable informations relative to the Fe^{3+} magnetic sublattices, in conjunction with those obtained by neutron diffraction. The angle Θ which is defined by the direction of the hyperfine field and that of the applied field (when parallel to the γ-beam), can be estimated from the relative integrated intensities A_i of the lines according to the following relationship

$$\Theta = \arcsin\sqrt{\frac{\frac{3}{2}\frac{A_{2,5}}{A_{1,6}}}{1+\frac{3}{4}\frac{A_{2,5}}{A_{1,6}}}} \tag{8}$$

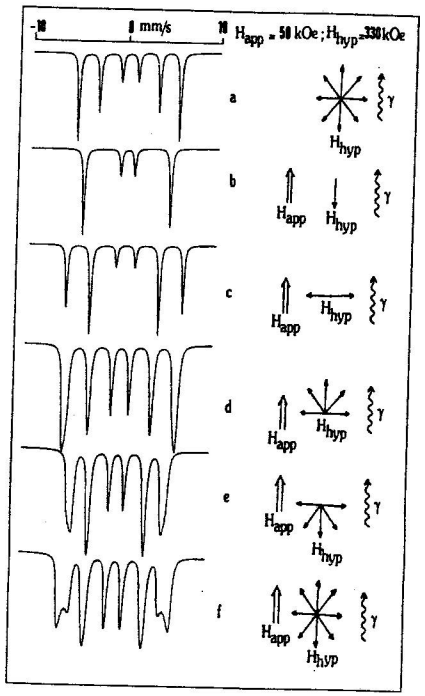

Figure 2: Theoretical Mössbauer spectra in various ideal situations (see text).

where $A_{1,6} = 3(1 + \cos^2\Theta)$ is the area of the outermost lines, $A_{2,5} = 4\sin^2\Theta$ of the intermediate lines and $A_{3,4} = 1 + \cos^2\Theta$ of the internal lines of the Zeeman sextet.

A second estimation of Θ can be obtained by considering the geometrical arrangement of the applied field, the effective field and the hyperfine field, as illustrated in figure 1, and its value is expressed as

$$\Theta = \arccos\left(\frac{H_{\rm eff}^2 - H_{\rm app}^2 - H_{\rm hyp}^2}{2H_{\rm app}H_{\rm hyp}}\right). \qquad (9)$$

The presence of sharp lines in the in-field Mössbauer spectrum is indicative of a well-defined orientation of the magnetic moments with respect to the applied field. An isotropic distribution of magnetic moments corresponds to the zero-field spectrum given in figure 2a, whereas figures 2b and 2c illustrate the case of ferromagnetic and antiferromagnetic systems under an applied field, respectively. Numerous spin alignment experiments were performed using HFMS: in ferrites, spinels, garnets, the different magnetic iron sublattices can be clearly identified as well as their respective orientations (see as examples [11, 12]). HFMS can also give direct evidence for spin reorientation [9] and

phase transitions induced by the applied field on easy axis single crystalline antiferromagnet [3, 13]. The situation is less clear in substituted ferrites because non collinear arrangements as localized canted state or Yafet-Kittel structure, have to be considered, as well as the substitution content [14].

On the contrary, the presence of broad lines is indicative of a lack of alignment of the magnetic moments (umbrella structures) under the influence of the applied field, due to the presence of single ion anisotropy, or the competition of antiferromagnetic interactions. As the lineshape reflects the vectorial addition of the applied field and the hyperfine field with its different orientations, the fitting of the spectrum requires a combined distribution of effective field and Θ angles $P(H_{\rm eff}, \Theta)$. Theoretical spectra expected for ideal spin structures so called sperimagnetic, asperimagnetic and speromagnetic are given in figures 2*d*, 2*e* and 2*f*, respectively. A speromagnet results from a randomly oriented spin freezing without preferred orientation, whereas the distribution of orientations is anisotropic with a preferred axis, in the case of an asperomagnet; a sperimagnet consists of a two-sublattices structure with one randomly oriented sublattice, both being ferro- or antiferromagnetically coupled [15, 16]. Let us mention finally that in presence of a quadrupole interaction (assumed axial), the dependence of the lines position with the effective field is more complex, because the angle defined by $H_{\rm eff}$ and V_{zz} (principal axis of [EFG]) varies with $H_{\rm app}$.

Besides the investigation of the magnetic arrangements, zero field and in- field Mössbauer experiments can also contribute to investigate the magnetic properties of ultra-fine particles. These magnetic systems are superparamagnetic, i.e. they behave as paramagnets below the "bulk" magnetic ordering temperatures (see a review of the superparamagnetism in [17] and HFMS applications in [5]). In that way, HFMS is able to provide some data concerning fundamental questions related to the structural aspects within the particles, the interparticle magnetic interactions as well as the surface effects. Let us mention that, according to a recent study, HFMS can also be used as a selective method of magnetic susceptibility measurements due to paramagnetic Mössbauer atoms [18].

3. HFMS applied to fluorides

In the present section, we report on HFMS experiments performed on some ferric fluorides where the Fe^{3+} cation occupies the center of an octahedral unit of fluorine. The values of the saturation hyperfine field in fluorides is well-defined; $H_{\rm hyp}^{\rm sat} = -62.5$T assuming $\mu(Fe^{3+}) = 5.0\mu_B$ and $H_{\rm hyp} = -25$T per spin unit. Let us note also that the hyperfine field is antiparallel to the Fe^{3+} magnetization. As the structures of transition metal fluorides results generally from packings of corner-sharing octahedral units, the values of the superexchange bond angle M-F-M favour antiferromagnetic couplings. These HFMS studies have been discussed in conjunction with neutron diffraction results and vice versa.

Among the numerous crystalline and amorphous compounds which have been investigated by HFMS, the best example is attributed to the simple ferric fluoride FeF_3. Three crystalline polymorphs of FeF_3 were synthetized up to now, as well as two varieties of amorphous phases (see [8, 9] and references therein). One can distinguish on

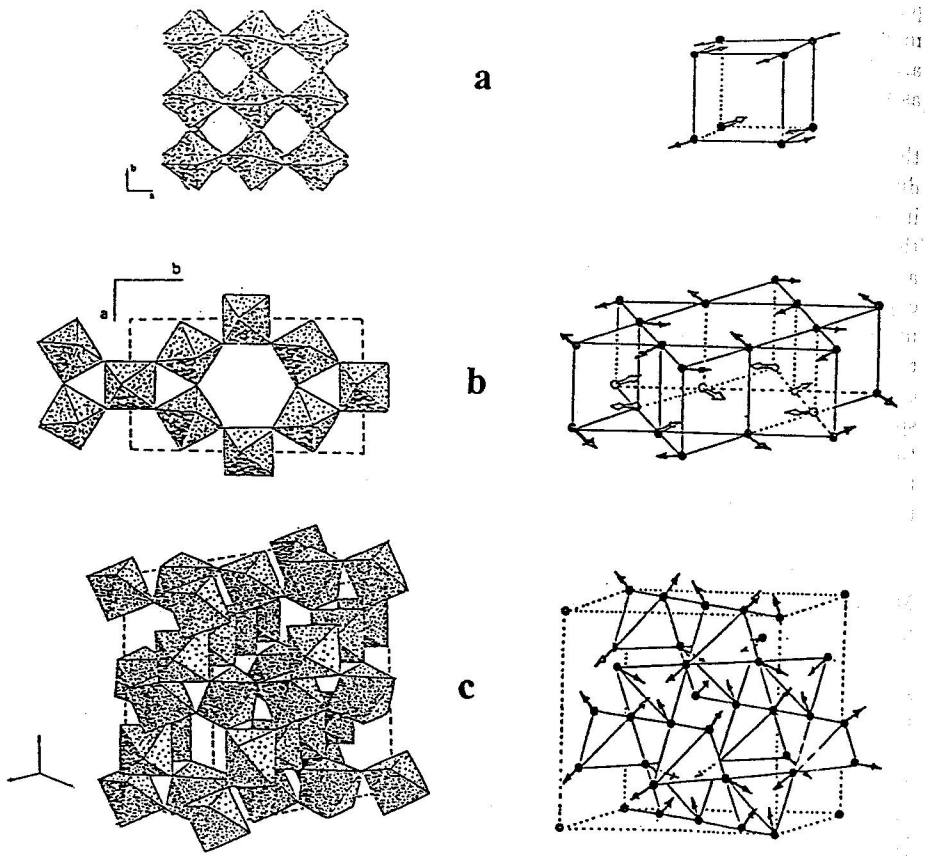

Figure 3: Crystal and magnetic structures of the three polymorphic crystalline forms of FeF_3: rhombohedral (a), hexagonal tungsten bronze (b), and pyrochlore (c).

figure 3 (a) the rhombohedral phase: its structure results from a pseudo-cubic packing of weakly tilted octahedral units and it orders as a weak ferromagnet below $T_N = 363K$; (b) the hexagonal tungsten bronze phase: it consists of the superposition of planes built up from hexagonal and triangular octahedral units rings and the magnetic structure ($T_N \approx 100K$) can be described as a 120 star planar arrangement with three ferromagnetic sublattices with antiferromagnetic coupling between planes; (c) the pyrochlore phase: the cationic lattice of this phase is built up from corner-sharing tetrahedra and below $T_N = 20K$, four ferromagnetic sublattices are arranged at 109° to each other because of the presence of triangular platelets. So, the magnetic arrangements at zero K and the magnetic characteristics (T_N, Θ_P) are quite different for these compounds

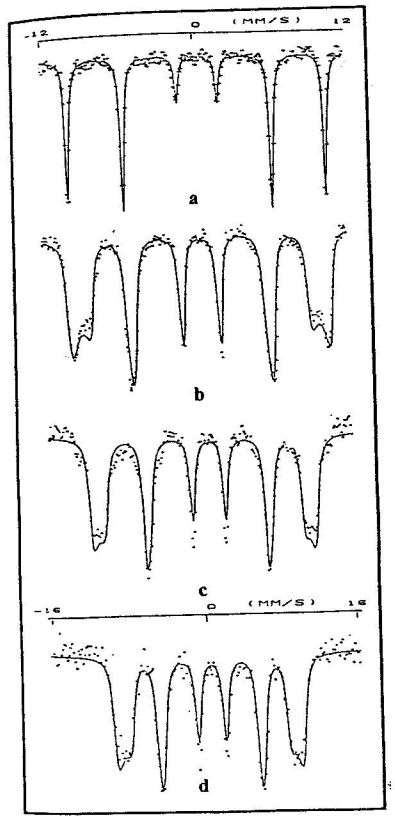

Figure 4: Powder in-field Mössbauer spectra recorded at 4.2K under an external magnetic field parallel to the γ-beam on rhombohedral (70kG) (a), hexagonal tungsten bronze (60kG) (b), pyroclore (40kG) (c) and the deposited amorphous (60kG) (d) of FeF_3.

and the changes can be explained in terms of frustration, taking into account their respective cationic topology which contains only triangular platelets [19, 20]. HFMS has revealed (i) the weak ferromagnetic behaviour of the rhombohedral phase as illustrated fig. 4a (the presence of a canting due to an asymmetric exchange interaction Dzyaloshinski-Moriya prevents from obtaining the spectrum expected for an ideal antiferromagnet, fig. 2c), (ii) the "speromagnetic-like" behaviour of the hexagonal and pyrochlore phases (fig. 4b and c, respectively) due to their rather complex magnetic structure resulting from the presence of Fe^{3+} triangular platelets [19, 20], and finally the speromagnetic behaviour of the amorphous varieties (fig. 4d) [21, 22]. In conjunction with structural data, this last result suggested that the structure of the ideal amorphous FeF_3 could be described by a continuous random packing of corner-sharing octahedra with no-dangling bonds [23, 24, 25], so that the presence of both odd and

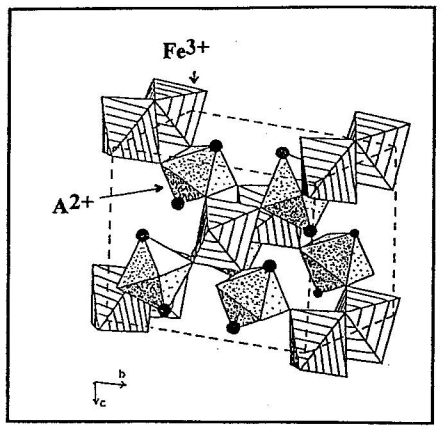

Figure 5: Perspective crystallographic view of the $AFeF_5(H_2O)_2$ weberite structure.

even-membered rings in the cationic topology is consistent with the magnetic properties [26].

Speromagnetic structures were also evidenced by HFMS on amorphous $AFeF_4$ samples with A= K, Rb, Cs, NH_4 [27]. More recently, magnetic spin cluster structures were evidenced from zero field and in-field experiments on the mixed fluoride series $Fe_{1-x}M_xF_3$ with M = Cr and V for appropriate substitution content [28, 29]. In this case, the competition between first and second nearest neighbours antiferromagnetic interactions (which cannot be neglected) gives rise to frustration, because of the occurence of triangular platelets in the cubic lattice [30].

The structure of the inverse weberite series ($AFeF_5$ $(H_2O)_2$, with A = Mn, Fe, Co or Ni) is made up of cationic triangles which originate frustration effects. A perspective view is presented on figure 5. This leads to three-dimensional frustrated ferrimagnets. In-field magnetic structures depend strongly on the nature of the divalent cation, essentially due to the magnetocrystalline anisotropy effect. The spectra recorded in a 80 kG applied field are illustrated in figure 6 as well as the schematic corresponding arrangements of the magnetic moments. Except for Mn-weberite spectrum, the others exhibit broad outermost lines due to a lack of orientations of the ferric magnetic moments (one can compare with ideal situations illustrated in figure 2). The fitting procedure consists in a combined distribution of Θ-angles and effective field to take into account of the line broadening (see details in [3]). Finally, it is found that the orientations of the Mn^{2+} and Fe^{3+} magnetic moments are consistent with a triangular magnetic lattice, because of the isotropic behavior of Mn^{2+}, whereas HFMS spectra have to be described from "asperomagnetic-like" and "sperimagnetic-like" models, in the case of Fe^{2+}, Co^{2+} and Ni^{2+} [31].

Low-dimensional structures were recently evidenced on the crystalline phases Pb_x-

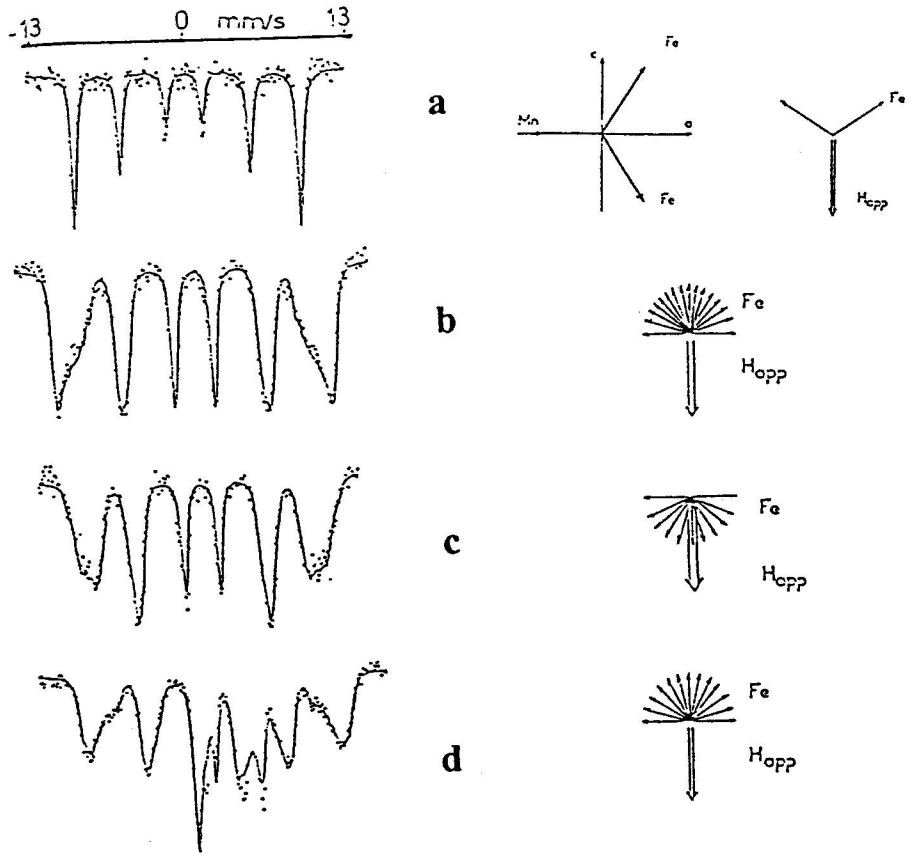

Figure 6: Powder in-field Mössbauer spectra recorded at 4.2K under a 80 kG applied field parallel to the γ-beam and corresponding schematic magnetic arrangements of the iron magnetic moments in $AFeF_5(H_2O)_2$ weberite compound with A= Mn (a), Co (b), Ni (c) and Fe (d).

$MM'F_{12}$, $3H_2O$ (with M = Mn^{2+}, Fe^{2+},and Fe^{3+}, M'=Fe^{3+}): they result from a triple infinite isolated chain of corner-sharing octahedra (see figure 7). The magnetic properties have been investigated by HFMS and neutron diffraction technique. The presence of triangular platelets within a chain originate triangular magnetic structures observed below the Néel temperature. The contribution of the weak interchain interactions which were evidenced at lower temperatures induces a canting of the magnetic moments and consequently increases the degree of magnetic frustration in these phases [32]. The first results of the magnetic structure show a nice agreement between HFMS and neutron diffraction studies. Further experiments are in progress, as well as numeric simulations.

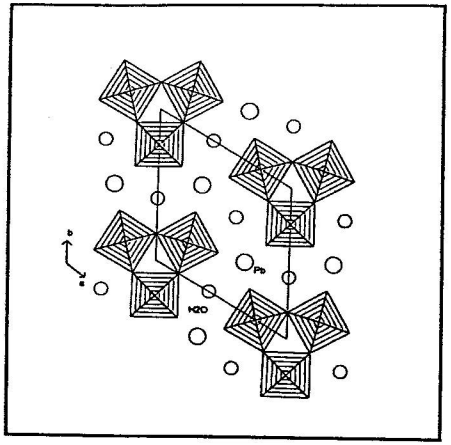

Figure 7: Projection in (001) plane of the crystal structure of $Pb_xMM'F_{12}$, $3H_2O$ (with M = Mn^{2+}, Fe^{2+}, and Fe^{3+}, M'=Fe^{3+}) phases.

4. Conclusions

rom these examples, one can conclude that HFMS is a valuable tool which contributes to the determination of the magnetic structures, essentially in the case of noncollinear arrangements. In most of the cases, neutron diffraction experiments have to be taken into account, in order to refine the magnetic structures. Let us note that the numeric simulation techniques have demonstrated their role in the predictions of the magnetic structures in addition to the experimental approach [33, 34]. Finally, the present knowledge of the magnetic properties of fluorides and the facilities provided by HFMS support actually new developments: mechanical milling was recently applied to some ferric fluorides as FeF_3 and Mössbauer studies are in progress.

References

[1] S.S.Hanna, J.Heberle, G.J.Perlow, R.S.Preston, D.H.Vincent: *Phys. Rev. Lett.* **4** (1960), 513;

[2] J.Chappert: *Journal de Physique C6* **35** (1974), 71;

[3] R.B.Frankel, *Mössbauer Effect Methodology*, edited by I.J. Gruverman, Plenum Press, New York, 9 (1974) 151

[4] J.Chappert, J.Teillet, F.Varret: *J. Magn. Magn. Mat.* **11** (1979), 200;

[5] Q.A.Pankhurst, R.J. Pollard, in *Mössbauer Spectroscopy Applied to Magnetism and Materials Science*, edited by G.J. Long and F. Grandjean, Plenum Press, New-York (1993) 77 and references therein

[6] J.M.D. Coey: *Can. J. Phys.* **65** (1987), 1210;

[7] K.Moorjani, J.M.D. Coey, in *Magnetic Glasses*, edited by S.P. Wolsky and A.W.Czanderna, Elsevier Amsterdam (1984)

[8] G. Ferey, M. Leblanc, J. Pannetier, R. de Pape, in *Inorganic Solid Fluorides*, edited by P. Hagenmuller, Academic Press, New-York, (1985) 395

[9] J.M. Greneche, F. Varret, in *Mössbauer Spectroscopy Applied to Magnetism and Materials Science*, edited by G.J. Long and F. Grandjean, Plenum Press, New-York (1993) 161

[10] G.Toulouse: *Commun. Phys.* **2** (1977), 115;

[11] J.Chappert, R.B. Frankel: *Phys. Rev. Lett.* **19** (1967), 570;

[12] L.K.Leung, B.J.Evans, A.H. Morrish: *Phys. Rev. B* **8** (1973), 29;

[13] C.E. Johnson, in *Mössbauer Spectroscopy Applied to Inorganic Chemistry*, edited by G.J. Long, Plenum Press, New-York, Vol 1 (1984) 619 and references therein

[14] J.L. Dormann, M. Nogues: *J. Phys.: Condensed Matter* **2** (1990), 1223;

[15] J.M.D. Coey, P.W. Readman: *Nature* **246** (1973), 476;

[16] C.M. Hurd: *Contemp. Phys.* **23** (1982), 469;

[17] J.L. Dormann: *Rev. Phys. Appl.* **16** (1981), 275;

[18] J.M. Greneche, J. Linares, F. Varret: *J. Phys.: Condensed Matter* **2** (1990), 4243;

[19] G. Ferey, R. de Pape, M. Leblanc, J. Pannetier: *Rev. Chim. Min.* **23** (1986), 674;

[20] Y. Calage, M. Zemirli, J.M. Greneche, F. Varret, R. De Pape, G. Ferey: *Journal of Solid State Chemistry* **69** (1987), 197;

[21] G. Ferey, F. Varret, J.M.D. Coey: *J. Phys. C: Solid State Phys.* **12** (1979), L531;

[22] M. Eibschutz, M.E. Lines, L.G. Van Uitert, M.J. Guggenheim, G.J. Zydzik: *Phys. Rev. B* **24** (1981), 2343; *ibid* **29** (1984), 3843;

[23] J.M. Greneche, A. Le Bail, M. Leblanc, A. Mosset, J. Galy, F. Varret, G. Ferey: *J. Phys. C: Solid State Phys.* **15** (1988), 1351;

[24] J.M.D. Coey, P.J.K. Murphy: *J. Non-Cryst. Solids* **50** (1982), 125;

[25] J.M. Greneche, J. Teillet, J.M.D. Coey: *J. Non-Cryst. Solids* **83** (1986), 27; *J. Phys.* **48** (1987), 1709;

[26] J.M. Greneche, J.M.D. Coey: *J. Phys.* **51** (1990), 231;

[27] M. Henry, F. Varret, J. Teillet, G. Ferey, O. Massenet, J.M.D. Coey: *J. Phys. C1* **41** (1980), 279;

[28] M. Lahlou-Mimi, Y. Pennec, J.M. Bassat, M. Leblanc, J.M. Greneche: *J. Magn. Magn. Mat.* **129** (1994), 289;

[29] M. Tamine, M. Leblanc, J.M. Greneche: *Hyperfine Interactions* **90** (1994), 417;

[30] M. Lahlou-Mimi, J.M. Greneche:*J. Magn. Magn. Mat.* (submitted);

[31] J.M. Greneche, J. Linares, F. Varret, Y. Laligant, G. Ferey: *J. Magn. Magn. Mat.* **73** (1988), 115;

[32] G. Decap, Y. Calage, J.M. Greneche, J. Rodriguez, *to be published*

[33] P. Lacorre, J. Pannetier: *J. Magn. Magn. Mat.* **71** (1987), 63;

[34] J. Linares, J.M. Greneche, F. Varret: *J. Phys.C: Solid State Phys.* **8** (1988), 901;